BBAA VI International Colloquium on:
Bluff Bodies Aerodynamics & Applications
Milano, Italy, July, 20-24 2008

STATISTICAL SYMMETRIES OF FLOW-INDUCED FORCES ON CYLINDERS

Luigi Carassale

Department of Civil Environmental and Architectural Engineering
University of Genova, Via Montallegro 1, 16145 Genova, Italy
e-mail: luigi.carassale@unige.it,

Keywords: Aerodynamics, cylinders in cross-flow, statistically-symmetric processes.

Abstract. *Aerodynamic tests on cylinder in cross-flow are often carried out in a nominally-symmetric configuration (e.g. symmetric cylinders with zero angle-of-attack). In such a condition, the pressure field and the fluid-induced forces acting on the cylinder are expected to fulfill some statistical symmetry condition, as it was experimentally observed by several researchers. In particular, it was noted that the cross-wind force and the torsional moment tend to have zero mean value and to be substantially uncorrelated with respect to the along-wind force. Small (but non-null) correlation or coherence values are often reported and it is not clear whether or not they should be treated as experimental imperfections or they are rather the trace of some physical phenomenon. With the objective of clarifying the mentioned problem, the present paper introduces the concept of statistically-symmetric random process presenting a definition in which the symmetry constraint is imposed on the characteristic functional. Consequent conditions on the statistical moments and on the covariance eigenfunctions are derived accordingly.*

1 INTRODUCTION

A very popular problem in experimental fluid-dynamics is constituted by the measurements of the fluid-induced forces acting on cylinders subjected to a cross flow produced in a wind tunnel. The global forces acting on the cylinder are originated by the unbalance of the pressure field acting on its surface, which, in turns, is related to the motion field of the fluid around it. The pressure field is randomly variable in time and space due to instabilities in the boundary layer and in the wake (if the Reynolds number in large enough) and due to the possible presence of turbulence in the incoming flow.

Typical experimental setups involve cylinders oriented in such a way to have a symmetry plane coincident to the symmetry plane of the test facility (e.g. vertical symmetric cylinders in a boundary-layer wind tunnel oriented at zero angle of attack). In such a condition, the pressure field is expected to fulfil some statistical symmetry condition, while, the statistics of the global forces should comply with some consequent restriction. It is known, for example, that, in this condition, the cross-wind force has zero mean value at any spanwise location along the cylinder and is uncorrelated with the along-wind force [1-4]. In practise, these results are not rigorously achieved and several authors documented the presence of non-null correlation or coherence between along-wind and cross-wind forces [5-7] or between along-wind force and torsional moment [5-8]. Such correlation or coherence values are often (but not always) small and it is not clear whether or not they should be treated as experimental inaccuracies or they are rather the trace of some physical phenomenon. The presence of such a weak (but non-null) correlation has small consequences on the evaluation of the global forces acting on the model, but, as it is shown in a case study presented herein, can deeply affect some statistical quantities often used for the interpretation of fluid-dynamic phenomena.

With the objective of clarifying the mentioned problem, the present paper introduces the concept of statistically-symmetric random process presenting a definition in which the symmetry constraint is imposed on the characteristic functional of the process. Starting from such a definition, the symmetry constraint on the statistical moments of the pressure field and of the forces-per-unit-length (FPUL) are derived. It is demonstrated that the covariance eigenfunctions of the pressure field are necessarily symmetric or antisymmetric and that the statistical moments of the FPUL must fulfil the relationship $\mathrm{E}[f_x^m\, f_y^n\, m_z^p]=0$ for $n+p$ odd, f_x, f_y, m_z being the along-wind force, the cross-wind force and the torsional moment. Also, it is demonstrated that the covariance eigenfunctions of the FPUL $\mathbf{f}(z)=[f_x(z)\ f_y(z)]^{\mathrm{T}}$, z being the span-wise abscissa, are oriented along the direction of the flow or orthogonal to it.

2 FLOW-INDUCED FORCES ON A PRISMATIC BODY: CASE STUDY

The present paragraph has mainly a motivational purpose and is intended as a summary of some notorious symmetry-related issues relevant in wind-tunnel tests. Some statistical properties of the flow-induced forces measured on a prismatic model tested in a boundary-layer wind tunnel are evaluated and discussed form a qualitative point of view, observing some well-known and intuitive behaviours, as well as some unusual an counterintuitive ones, which though they were reported in the technical literature, did not received any theoretical explanation. The model (Fig. 1) representing a square-base high-rise building, is instrumented by 500 pressure taps uniformly distributed on its lateral surface and simultaneously acquired in such a way to estimate the instantaneous pressure field acting on the model. The values measured by all the pressure channels are referred to a common reference pressure corresponding to the wind-tunnel static pressure at the test section. The referred test was carried out at the Shimizu Corporation Laboratories and further details can be found in [9].

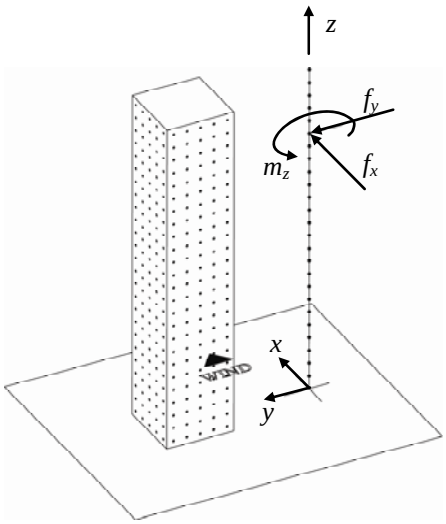

Figure 1. Case study: experimental setup.

Let f_x and f_y be, respectively, the along-wind and cross-wind FPUL acting on the model, evaluated integrating the pressure field at each instrumented level. The statistics of the FPUL are estimated from the data, assuming that the pressure field is a stationary and ergodic random process, by averaging the instantaneous values measured throughout the whole test.

Figure 2a shows the mean value of the along-wind FPUL, $\mu_{f_x}(z_j)$ (nondimensionalised by $0.5\rho bU^2$, ρ being the air density, b the side of the cylinder and U the incoming mean wind velocity), evaluated at the 25 instrumented levels z_j (j=1,…,25) of the model averaging a number of samples ranging form 1 to 3×10^4; as the number of samples increases, the plots quickly converge to stable values, which are greater for higher levels due to the mean-velocity profile in the boundary layer. Exception to this behaviour are levels j=1 and j=25, respectively, at the base and at the top of the cylinder. Figure 2b shows the mean value of the cross-wind FPUL, $\mu_{f_y}(z_j)$, nondimensionalised by the along-wind FPUL at the corresponding level; as the number of samples increases, μ_{f_y} rapidly converge to levels constituting a few percent of the along-wind forces. Such values are interpreted as experimental errors due to imperfections in the instrument calibration or in the wind-tunnel flow characteristics and are often corrected by fine-tuning the experimental setup. Figures 2c,d,e show the root mean square (rms) of along-wind (σ_{f_x}, Fig. 2c) and cross-wind (σ_{f_y}, Fig. 2d) FPUL, as well as their correlation coefficient ($\rho_{f_x f_y}$, Fig. 2e), versus the number of samples included in the average. The rms of both the FPUL are nondimensionalised by the mean value of the along-wind FPUL at the corresponding level. All the three mentioned quantities have a fast convergence to statistically stable values; the correlation coefficients converge to small values that, again, are interpreted as consequences of experimental imperfections.

The quantities described above are very basic tools for the analysis of flow-induced forces, their derivation from the data is straightforward, and it is not surprising to see some evident consequence of symmetry ($\mu_{f_y}\simeq0$, $\rho_{f_x f_y}\simeq0$). However, for other statistical quantities widely used in practice, the situation is rather more complicate. As an example, let us consider the vector of the FPUL $\mathbf{f}(z) = [f_x(z)\ f_y(z)]^{\mathrm{T}}$ and its two-point covariance function $\mathbf{C_{ff}}(z_1,z_2)$. Let $\boldsymbol{\phi}_k(z)$ be an eigenfunction of $\mathbf{C_{ff}}$, i.e. a solution of the integral equation:

$$\int_0^h \mathbf{C_{ff}}(z_1,z_2)\boldsymbol{\phi}_k(z_2)\,\mathrm{d}z_2 = \lambda_k\boldsymbol{\phi}_k(z_1) \qquad z_1\in[0,h],\quad k=1,2,... \tag{1}$$

and λ_k the corresponding eigenvalue. The eigenfunctions $\boldsymbol{\phi}_k(z)$ are functions in $\mathbb{R}^2$ and can be used as a base to represent $\mathbf{f}(z)$ as:

$$\mathbf{f}(z) = \boldsymbol{\mu}_{\mathbf{f}}(z) + \sum_{k=1}^{\infty} \boldsymbol{\phi}_k(z)\, x_k \tag{2}$$

where $\boldsymbol{\mu}_{\mathbf{f}}(z)$ is the mean value of $\mathbf{f}(z)$ and x_k are uncorrelated random variables whose variance is provided by the eigenvalues λ_k. The spectral representation expressed by Eq. (2) is referred to as Proper Orthogonal Decomposition (POD) and is widely employed in many scientific fields including fluid-dynamics and bluff-body aerodynamics [e.g. 9, 10]. The eigenfunctions $\boldsymbol{\phi}_k(z)$ are generally used as a tool for identifying coherent structures in random processes and, in the present case, they may represent typical patterns of the fluctuating part of the FPUL.

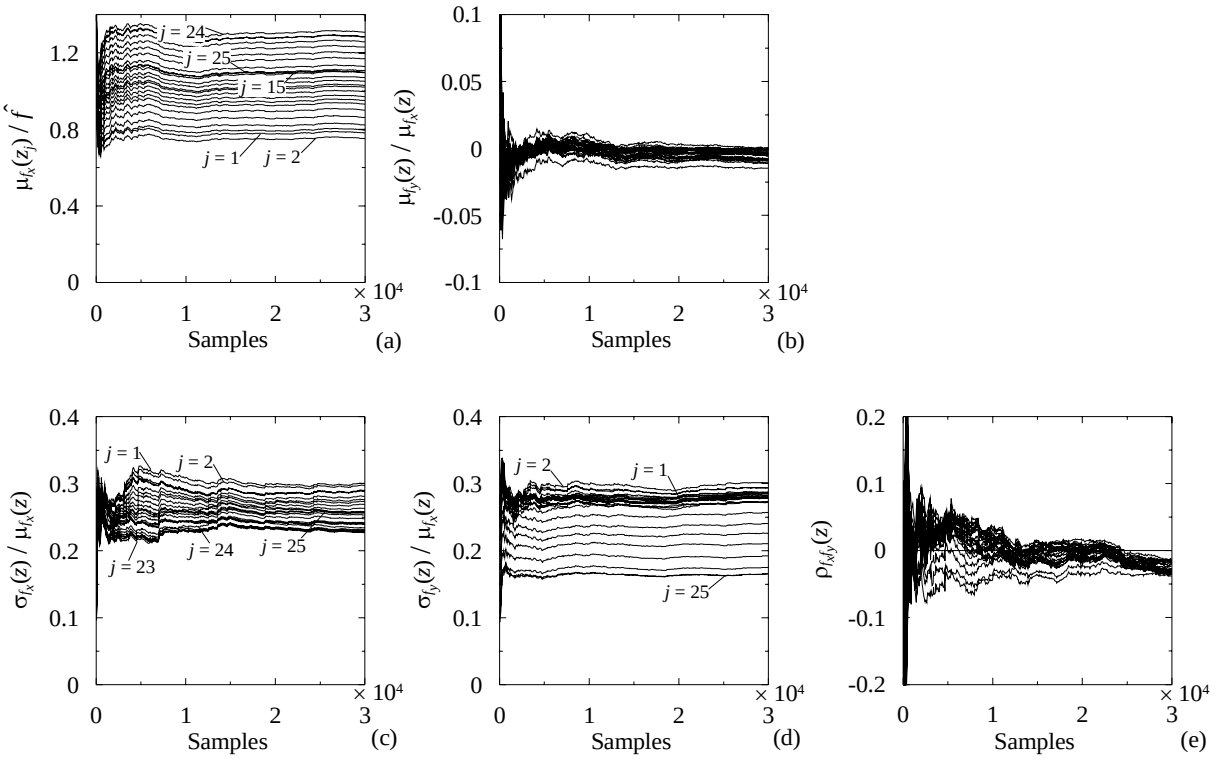

Figure 2. Single-point statistics of FPUL vs number of samples. Mean along-wind (a) and cross-wind (b) FPUL; Rms along-wind (c) and cross-wind (d) FPUL; correlation coefficient along-wind and cross-wind FPUL (e).

Let $\varphi_k(z)$ be the angle in the x-y plane of the vector $\boldsymbol{\phi}_k(z)$ with respect to the x-axis. Figure 3 shows the angle $\varphi_1(z)$ evaluated at each instrumented level of the model and for different number of samples. It suggests that the most powerful coherent component of the FPUL acts in a plane oriented in somehow (by the angle φ_1) between the axes x and y. This is clearly strange for a process that is expected to be symmetric in some way. As it will be shown in the following, this behaviour is not necessarily related to physical causes, but may be due to the sensitivity of $\boldsymbol{\phi}_1$ to lacks of symmetry of the pressure field as it can be argued noting that the angles φ_1 have wide statistical fluctuations.

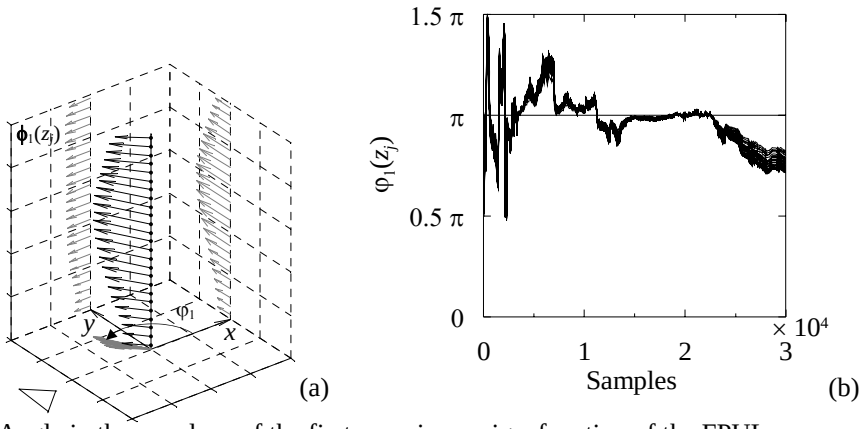

Figure 3. Angle in the *x*-*y* plane of the first covariance eigenfunction of the FPUL.

3 PROPERTIES OF A STATISTICALLY-SYMMETRIC PRESSURE FIELD

Let $q(s,z)$ be the fluid-induced pressure acting on the cylinder surface in a cross-section with spanwise abscissa z and in a point of the cross-section border defined by the curvilinear abscissa s (Fig. 4). The pressure q is modeled as a random process, which can be completely represented by its characteristic functional:

$$\psi_q\left[\theta(s,z)\right] = \mathrm{E}\left[\exp\left(\mathrm{i}\int_0^h\int_{-c/2}^{c/2}\theta(s,z)\,q(s,z)\,\mathrm{d}s\,\mathrm{d}z\right)\right] \tag{3}$$

where h is the height of the model, c is the length of the cross-section border and i is the imaginary unit; the argument function $\theta(s,z)$ is supposed to be absolutely-integrable in $[-c/2, c/2]\times[0, h]$. A quite reasonable definition of statistical symmetry can be defined on such a basis: the process $q(s,z)$ is referred to as a statistically-symmetric random process (SSRP) with respect to s if its characteristic functional is invariant for a reflection of the coordinate s, i.e.:

$$\psi_q\left[\theta(-s,z)\right] = \psi_q\left[\theta(s,z)\right] \qquad \forall z\in[0,h] \tag{4}$$

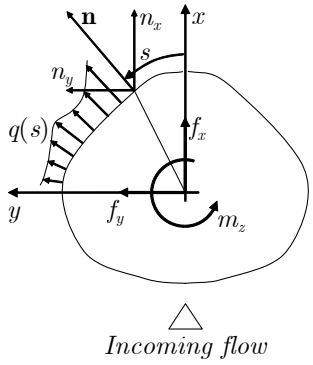

Figure 4. Flow-induced pressure and FPUL on a cylinder cross-section.

In order to evaluate the consequences of such an assumption on the statistical properties of the pressure field, let us assume that (almost all) the realizations of the process $q(s)$ are regular enough to be represented by the (generalized) Fourier series expansion:

$$q(s,z) \simeq \left(\mathbf{M}(s) \otimes \mathbf{H}(z)\right)^{\mathrm{T}} \mathbf{a} + \left(\mathbf{N}(s) \otimes \mathbf{H}(z)\right)^{\mathrm{T}} \mathbf{b} \tag{5}$$

where $\otimes$ represents the Kronecker product; $\mathbf{M}(s)$ and $\mathbf{N}(s)$ are n_s-order vectors collecting, respectively, the even and the odd terms of the Fourier functional basis in [–c/2, c/2], while $\mathbf{H}(z)$ is an n_z-order vector containing the n_z more representative elements of an orthogonal basis in $L^2([0,h])$. The vectors $\mathbf{a}$ and $\mathbf{b}$ are random vectors of dimension $n_s n_z$ containing the Fourier coefficients of the process q:

$$\mathbf{a} = \int_0^h \int_{-c/2}^{c/2} \left(\mathbf{M}(s) \otimes \mathbf{H}(z)\right) q(s,z)\,\mathrm{d}s\,\mathrm{d}z; \qquad \mathbf{b} = \int_0^h \int_{-c/2}^{c/2} \left(\mathbf{N}(s) \otimes \mathbf{H}(z)\right) q(s,z)\,\mathrm{d}s\,\mathrm{d}z \tag{6}$$

The elements of the vectors $\mathbf{M}(s)$, $\mathbf{N}(s)$ and $\mathbf{H}(z)$ are scaled in such a way to fulfill the orthonormality properties:

$$\begin{aligned} &\int_{-c/2}^{c/2} \mathbf{M}(s)\mathbf{M}(s)^{\mathrm{T}}\,\mathrm{d}s = \mathbf{I}_{n_s}; \quad \int_{-c/2}^{c/2} \mathbf{N}(s)\mathbf{N}(s)^{\mathrm{T}}\,\mathrm{d}s = \mathbf{I}_{n_s}; \quad \int_0^h \mathbf{H}(z)\mathbf{H}(z)^{\mathrm{T}}\,\mathrm{d}z = \mathbf{I}_{n_z}; \\ &\int_{-c/2}^{c/2} \mathbf{M}(s)\mathbf{N}(s)^{\mathrm{T}}\,\mathrm{d}s = \mathbf{0} \end{aligned} \tag{7}$$

where $\mathbf{I}_n$ is the n-order identity matrix and $\mathbf{0}$ is the null matrix.

Substituting Eq. (5) into Eq. (3), the characteristic functional of the process q can be approximate by the expression:

$$\psi_q\left[\theta(s,z)\right] \simeq \mathrm{E}\left[\exp\left(\mathrm{i}\,\boldsymbol{\alpha}^{\mathrm{T}}\mathbf{a} + \mathrm{i}\,\boldsymbol{\beta}^{\mathrm{T}}\mathbf{b}\right)\right] = \psi_{\mathbf{a},\mathbf{b}}(\boldsymbol{\alpha},\boldsymbol{\beta}) \tag{8}$$

where $\boldsymbol{\alpha}$ and $\boldsymbol{\beta}$ are deterministic vectors of dimension $n_s n_z$ containing, respectively, the even and odd the Fourier coefficients of the argument function $\theta(s,z)$, i.e.:

$$\boldsymbol{\alpha} = \int_0^h \int_{-c/2}^{c/2} \left(\mathbf{M}(s) \otimes \mathbf{H}(z)\right) \theta(s,z)\,\mathrm{d}s\,\mathrm{d}z; \qquad \boldsymbol{\beta} = \int_0^h \int_{-c/2}^{c/2} \left(\mathbf{N}(s) \otimes \mathbf{H}(z)\right) \theta(s,z)\,\mathrm{d}s\,\mathrm{d}z \tag{9}$$

and $\psi_{\mathbf{a},\mathbf{b}}$ is the joint characteristic function of the random vectors $\mathbf{a}$ and $\mathbf{b}$.

The symmetry condition imposed on the process q (Eq. (4)) assures, through Eqs. (8) and (9), that the characteristic function $\psi_{\mathbf{a},\mathbf{b}}$ fulfils the relationship:

$$\psi_{\mathbf{a},\mathbf{b}}(\boldsymbol{\alpha},-\boldsymbol{\beta}) = \psi_{\mathbf{a},\mathbf{b}}(\boldsymbol{\alpha},\boldsymbol{\beta}) \tag{10}$$

i.e. it is invariant for a reflection of the odd-Fourier-coefficient vector $\boldsymbol{\beta}$. This condition has consequences on the joint statistical moments of the vectors $\mathbf{a}$ and $\mathbf{b}$, which can be obtained, by differentiation, from their characteristic function, yielding:

$$\nabla_{\boldsymbol{\alpha}}^{[m]} \otimes \nabla_{\boldsymbol{\beta}}^{[n]} \otimes \psi_{\mathbf{a},\mathbf{b}}\Big|_{\mathbf{0},\mathbf{0}} = \mathrm{i}^{m+n}\,\mathrm{E}\left[\mathbf{a}^{[m]} \otimes \mathbf{b}^{[n]}\right] = \mathrm{i}^{m-n}\,\mathrm{E}\left[\mathbf{a}^{[m]} \otimes \mathbf{b}^{[n]}\right] \qquad (n,m = 0,1,\ldots) \tag{11}$$

where $\bullet^{[p]}$ is the p-time-iterated Kronecker product and $\nabla_{\mathbf{x}} = [\partial/\partial x_1 \ \ldots \ \partial/\partial x_r]^{\mathrm{T}}$ is the vector containing the r partial derivative operators with respect to the components of the r-order vector $\mathbf{x}$. Eq. (11) implies that for any odd n, the expectation must vanish, i.e. all the statistical moments containing an odd number of $\mathbf{b}$'s must be null:

$$\mathrm{E}\left[\mathbf{a}^{[m]} \otimes \mathbf{b}^{[n]}\right] = \mathbf{0} \qquad \text{if } n \text{ is odd} \tag{12}$$

3.1 Forces per unit length

The generalized FPUL (along-wind force f_x, cross-wind force f_y and torsional moment m_z) acting on the cylinder at the spanwise abscissa z are calculated by integrating the pressure field $q = q(s,z)$ over the cross-section border as:

$$\begin{aligned} f_x(z) &= \int_{-c/2}^{c/2} n_x(s)\, q(s,z)\mathrm{d}s \\ f_y(z) &= \int_{-c/2}^{c/2} n_y(s)\, q(s,z)\mathrm{d}s \\ m_z(z) &= \int_{-c/2}^{c/2} \left(x(s)n_y(s) - y(s)n_x(s)\right) q(s,z)\,\mathrm{d}s \end{aligned} \tag{13}$$

where n_x and n_y are the Cartesian components of a unit vector normal to the border $\mathbf{n}=\mathbf{n}(s)$ in the point with abscissa s and coordinates $x(s)$ and $y(s)$ (Fig. 4). Since the functions n_x and n_y are, respectively, symmetric and anti-symmetric with respect to s and due to the orthonormality properties offered by Eqs. (7), the FPUL can be approximated by the expression:

$$\mathbf{f}(z) = \begin{bmatrix} f_x(z) \\ f_y(z) \\ m_z(z) \end{bmatrix} = \left(\begin{bmatrix} \boldsymbol{\gamma}_x & \mathbf{0} & \mathbf{0} \\ \mathbf{0} & \boldsymbol{\gamma}_y & \boldsymbol{\gamma}_z \end{bmatrix} \otimes \mathbf{H}(z) \right)^{\mathrm{T}} \begin{bmatrix} \mathbf{a} \\ \mathbf{b} \end{bmatrix} \tag{14}$$

where $\boldsymbol{\gamma}_x$, $\boldsymbol{\gamma}_y$, and $\boldsymbol{\gamma}_z$ are deterministic vectors depending on the shape of the cross-section as:

$$\boldsymbol{\gamma}_x = \int_{-c/2}^{c/2} \mathbf{M} n_x \,\mathrm{d}s; \qquad \boldsymbol{\gamma}_y = \int_{-c/2}^{c/2} \mathbf{N} n_y \,\mathrm{d}s; \qquad \boldsymbol{\gamma}_z = \int_{-c/2}^{c/2} \mathbf{N}\left(x n_y - y n_x\right)\mathrm{d}s \tag{15}$$

According to the representation provided by Eq. (14), the joint characteristic function of the generalized FPUL $f_x(z_1)$, $f_y(z_2)$ and $m_z(z_3)$, z_1, z_2, z_3 being three values of the spanwise abscissa, can be expressed as:

$$\begin{aligned} \psi_{f_x,f_y,m_z}(\varphi_x,\varphi_y,\mu_z) &= \mathrm{E}\Big[\exp\Big(\mathrm{i}\varphi_x \left(\boldsymbol{\gamma}_x \otimes H(z_1)\right)^{\mathrm{T}} \mathbf{a} + \mathrm{i}\varphi_y \left(\boldsymbol{\gamma}_y \otimes H(z_2)\right)^{\mathrm{T}} \mathbf{b} + \\ &\qquad + \mathrm{i}\mu_z \left(\boldsymbol{\gamma}_z \otimes H(z_3)\right)^{\mathrm{T}} \mathbf{b} \Big) \Big] \\ &= \psi_{\mathbf{a},\mathbf{b}} \left(\varphi_x \left(\boldsymbol{\gamma}_x \otimes H(z_1)\right), \varphi_y \left(\boldsymbol{\gamma}_y \otimes H(z_2)\right) + \mu_z \left(\boldsymbol{\gamma}_z \otimes H(z_3)\right) \right) \end{aligned} \tag{16}$$

and their statistical moments result:

$$\begin{aligned} \mathrm{E}\left[f_x^m(z_1)\, f_y^n(z_2)\, m_z^p(z_3) \right] &= \frac{1}{\mathrm{i}^{m+n+p}} \left. \frac{\partial^{m+n+p} \psi_{f_x(z_1),f_y(z_2),m_z(z_3)}}{\partial\varphi_x^m \partial\varphi_y^n \partial\mu_z^p} \right|_{0,0,0} = \\ &= \left(\left(\boldsymbol{\gamma}_x \otimes \mathbf{H}(z_1)\right)^{[n]} \otimes \left(\boldsymbol{\gamma}_y \otimes \mathbf{H}(z_2)\right)^{[m]} \otimes \left(\boldsymbol{\gamma}_z \otimes \mathbf{H}(z_3)\right)^{[p]} \right)^{\mathrm{T}} \mathrm{E}\left[\mathbf{a}^{[m]} \otimes \mathbf{b}^{[n+p]} \right] \end{aligned} \tag{17}$$

from which, according to Eq. (12), it can be concluded that:

$$\mathrm{E}\left[f_x^m(z_1)\, f_y^n(z_2)\, m_z^p(z_3) \right] = 0 \quad \text{if } n+p \text{ is odd}, \qquad \left(z_1, z_2, z_3 \in [0,h]\right) \tag{18}$$

Eq. (18) states that all the cross statistical moments of the FPUL involving cross-wind force and torsional moment with exponents whose sum is odd necessarily vanish.

Rewriting Eq. (17) for $m + n + p = 2$, adopting the ordinary matrix product and introducing the symmetry constraint given by Eq. (12), the two-point covariance matrix of the FPUL vector can be expressed as:

$$\mathbf{C_{ff}}(z_1, z_2) = \begin{pmatrix} \left(\boldsymbol{\gamma}_x \otimes \mathbf{H}(z_1)\right)^{\mathrm{T}} \mathbf{C_{aa}} \left(\boldsymbol{\gamma}_x \otimes \mathbf{H}(z_2)\right) & \mathbf{0} \\ \mathbf{0} & \left(\left[\boldsymbol{\gamma}_y \;\; \boldsymbol{\gamma}_z\right] \otimes \mathbf{H}(z_1)\right)^{\mathrm{T}} \mathbf{C_{bb}} \left(\left[\boldsymbol{\gamma}_y \;\; \boldsymbol{\gamma}_z\right] \otimes \mathbf{H}(z_2)\right) \end{pmatrix} \tag{19}$$

where $\mathbf{C_{aa}}$ and $\mathbf{C_{bb}}$ are the covariance matrices of the vectors **a** and **b**, respectively. Using such representation, the eigenvalue problem defined by Eq. (1) can be converted into the two coupled problems:

$$\begin{cases} \left(\boldsymbol{\gamma}_x \otimes \mathbf{H}(z_1)\right)^{\mathrm{T}} \mathbf{C_{aa}} \displaystyle\int_0^h \left(\boldsymbol{\gamma}_x \otimes \mathbf{H}(z_2)\right) \phi_k^{(x)}(z_2)\, \mathrm{d}z_2 = \lambda_k \phi_k^{(x)}(z_1) \\ \left(\left[\boldsymbol{\gamma}_y \quad \boldsymbol{\gamma}_z\right] \otimes \mathbf{H}(z_1)\right)^{\mathrm{T}} \mathbf{C_{bb}} \displaystyle\int_0^h \left(\left[\boldsymbol{\gamma}_y \quad \boldsymbol{\gamma}_z\right] \otimes \mathbf{H}(z_2)\right) \boldsymbol{\phi}_k^{(y,z)}(z_2)\, \mathrm{d}z_2 = \lambda_k \boldsymbol{\phi}_k^{(y,z)}(z_1) \end{cases} \quad \begin{matrix} z_1 \in [0,h] \\ k = 1,2,\ldots \end{matrix} \tag{20}$$

in which the eigenfunctions $\boldsymbol{\phi}_k(z)$ have been partitioned into a scalar-valued component $\phi_k^{(x)}(z)$ for the along-wind direction and an $\mathbb{R}^2$-valued component $\boldsymbol{\phi}_k^{(y,z)}(z)$ relevant to cross-wind force and torsional moment. Left-multiplying Eqs. (20) by $\mathbf{H}(z_1)$ and integrating for z_1 over $[0, h]$, it results:

$$\begin{cases} \left(\boldsymbol{\gamma}_x \otimes \mathbf{I}_{n_z}\right)^{\mathrm{T}} \mathbf{C_{aa}} \left(\boldsymbol{\gamma}_x \otimes \mathbf{I}_{n_z}\right) \hat{\boldsymbol{\phi}}_h^{(x)} = \lambda_h \hat{\boldsymbol{\phi}}_h^{(x)} \\ \left(\left[\boldsymbol{\gamma}_y \quad \boldsymbol{\gamma}_z\right] \otimes \mathbf{I}_{n_z}\right)^{\mathrm{T}} \mathbf{C_{bb}} \left(\left[\boldsymbol{\gamma}_y \quad \boldsymbol{\gamma}_z\right] \otimes \mathbf{I}_{n_z}\right) \hat{\boldsymbol{\phi}}_h^{(y,z)} = \lambda_h \hat{\boldsymbol{\phi}}_h^{(y,z)} \end{cases} \qquad h = 1, \ldots, 3n_z \tag{21}$$

where $\hat{\boldsymbol{\phi}}_h^{(x)}$ and $\hat{\boldsymbol{\phi}}_h^{(y,z)}$ are vectors with size n_z- and $2n_z$, respectively, containing the Fourier coefficients of the eigenfunctions $\phi_k^{(x)}(z)$ and $\boldsymbol{\phi}_k^{(y,z)}(z)$, i.e.:

$$\phi_h^{(x)}(z) = \mathbf{H}^{\mathrm{T}}(z) \hat{\boldsymbol{\phi}}_h^{(x)}; \qquad \boldsymbol{\phi}_h^{(y,z)}(z) = \left(\mathbf{I}_2 \otimes \mathbf{H}(z)\right)^{\mathrm{T}} \hat{\boldsymbol{\phi}}_h^{(y,z)} \tag{22}$$

Eq. (22) demonstrates that, if the two eigenvalue problems in Eq. (21) have no common eigenvalues, then the eigenfunctions $\boldsymbol{\phi}_h(z)$ must contain only alternatively along-wind or cross-wind / torsional components. The symmetry condition does not allow hybrid along-wind / cross-wind or along-wind / torsional eigenfunctions.

4 DISCUSSION OF EXPERIMENTAL RESULTS

In the present Section, some results of the experiment described in Section 2 are reported and commented pointing out the effects of the slight lack of symmetry present in the measured data. Let $q(s,z)$ be the measured pressure non-dimensionalised by the mean dynamic pressure evaluated at the top of the model. All the statistical quantities are evaluated by time-averaging a single experiment record including 2^{16} samples per channel.

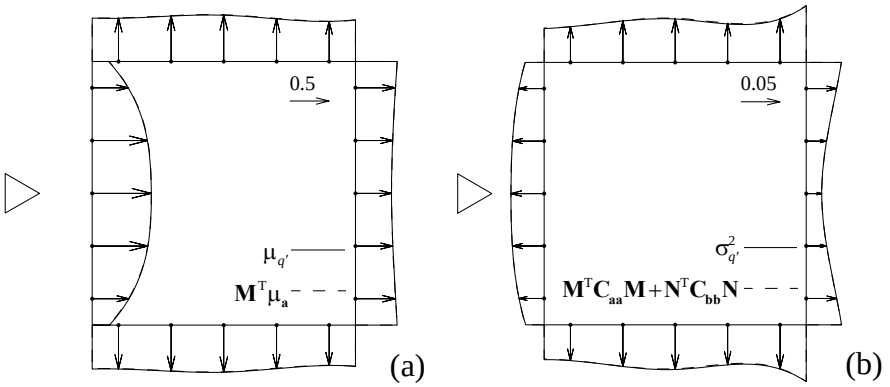

Figure 5. Pressure on the model surface at z=0.6 h: (a) measured mean value (solid line) and symmetrized mean value (dashed line); (b) measured variance (solid line) and symmetrized variance (dashed line).

Figure 5 shows the mean (a) and the variance (b) of the pressure measured on the model at z = 0.6 h (solid line), compared with the corresponding statistics obtained representing the pressure field by Eq. (5) and imposing the symmetry constraints E[**b**]=**0**, E[**ab**^{T}]=**0** (dashed lines, practically coincident with solid lines).

Figure 6 shows the covariance eigenfunctions of the FPUL $\mathbf{f}(z)=[f_x(z)\ f_y(z)]^T$ estimated from the measured data by Eq. (1) (Figs. 6a.1 – 6a.4) and obtained through the expressions given by Eqs. (21) and (22) implying the statistical symmetry of the pressure field (Figs. 6b.1 – 6b.4). Figure 7 shows the covariance eigenvalues of the measured FPUL (+ symbol) and the sorted sequence of the eigenvalues of corresponding to the along-wind ($\lambda_h^{(x)}$, □ symbol) and the cross-wind ($\lambda_h^{(y)}$, ▷ symbol) eigenfunctions provided by Eqs. (21). The first two eigenfunctions obtained from the data ($\boldsymbol{\phi}_1$ and $\boldsymbol{\phi}_2$, Figs. 6a.1 and 6a.2) represent hybrid along-wind / cross-wind modes and do not comply with the symmetry condition prescribing that the eigenfunctions should be necessarily oriented along the x-axis ($\boldsymbol{\phi}_1^{(x)}$, Fig. 6b.2) or along the y-axis ($\boldsymbol{\phi}_1^{(y)}$, Fig. 6b.1). It could be demonstrated (but it appears quite clear form the observation of Figure 6) that the two eigenfunctions $\boldsymbol{\phi}_1$ and $\boldsymbol{\phi}_2$ span approximately the same subspace as the two eigenfunctions $\boldsymbol{\phi}_1^{(x)}$ and $\boldsymbol{\phi}_1^{(y)}$. The eigenfunctions are individually different due to a small lack of symmetry in the measured data whose effect is emphasised by the fact that the first two eigenvalues are very close each other. This is confirmed by the fact that the eigenfunctions $\boldsymbol{\phi}_3$ and $\boldsymbol{\phi}_4$, for which the gap between the corresponding eigenvalues is substantially greater, perfectly comply with the symmetry constraint.

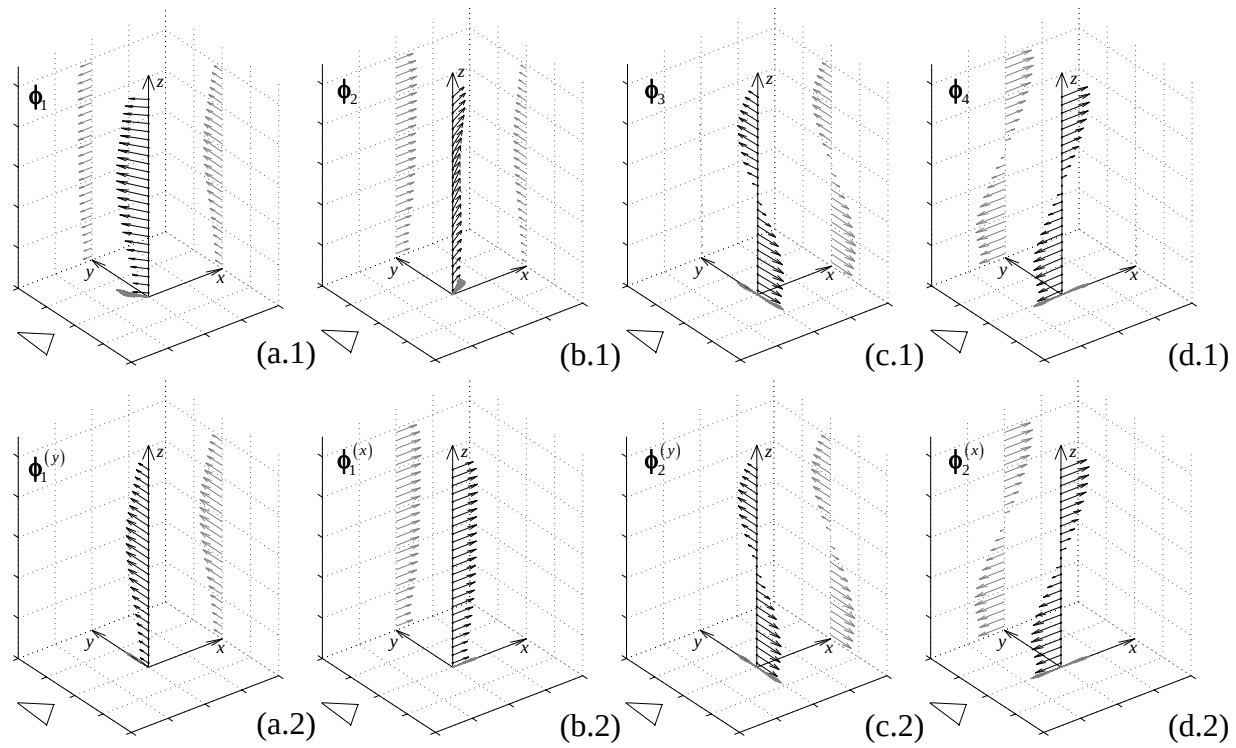

Figure 6. First four covariance eigenfunctions of the FPUL (along-wind and cross-wind) estimated from the measured data (a.1 – a.4) and corresponding eigenfunctions obtained through Eqs. (21) and (22) implying the statistical symmetry of the pressure field.

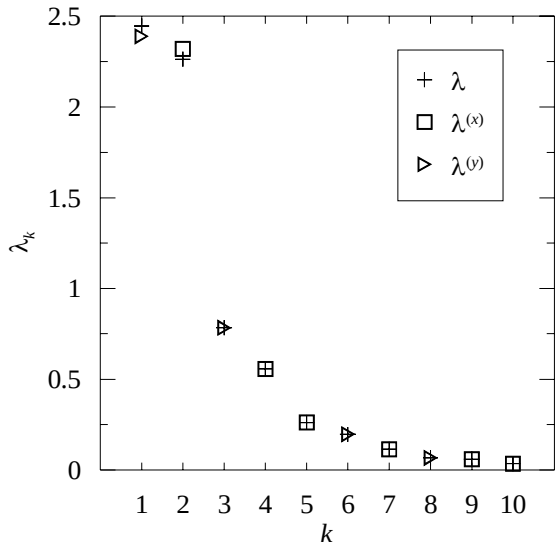

Figure 7. Covariance eigenvalues of the measured FPUL (+ symbol); eigenvalues corresponding to the along-wind ($\lambda_h^{(x)}$, □ symbol) and the cross-wind ($\lambda_h^{(y)}$, ▷ symbol) eigenfunctions provided by Eqs. (21).

5 CONCLUSIONS

When an aerodynamic test is carried out in nominally-symmetric conditions, it seems quite reasonable to assume that the pressure field (and, in general, all the flow-related quantities in the neighbourhood of the body) fulfil a statistical symmetry of the type described in Section 3. If it is true, it has been demonstrated that the statistical properties of the pressure field, as well

as of the FPUL must comply with some specific restrictions. Obviously, this does not rigorously happen for measured data, which are necessarily contaminated by some lack-of-symmetry due to imperfections in the experimental setup, inaccuracy in the measurements or insufficient statistical sampling. It has been observed that this (usually) small lack-of-symmetry may lead to the estimation of some statistical quantities that are significantly non-compliant with the symmetry constraint, likewise in the case of covariance eigenvectors, and may suggest erroneous interpretations of the observed phenomenon.

When the lack-of-symmetry is weak and is likely to be related to small experimental inaccuracies, the aforementioned problem can be circumvented forcing the symmetry by correcting the statistics (neglecting the non-symmetrical terms) or by suitably adjusting the measured data. It must be noted, however, that some particular cases do exist in which experimental results may appear as affected by large lack-of-symmetry even if the experimental setup is a nominally symmetric one (e.g. a large steady lift force for symmetric cylinders). This happens since stationarity and ergodicity are often invoked by researchers in order to estimate statistics from a necessarily limited number of experiment runs, but are not necessarily complied by the physics of the problem. While stationarity is practically fulfilled once the observation time is long enough (and a sufficient time for the stabilisation of the wind tunnel is allowed), ergodicity may be violated due to the possible existence of concurrent stable flow configurations triggered by random events (it is the case, for example, of circular cylinders in the neighbourhood of the critical Reynolds number, which may have a single stable recirculation bubble appearing randomly at one side of the cylinder (e.g. [11]). Concerning with these cases, it is worth noting that the statistical-symmetry condition defined herein is bases on the ensemble-averaging of the data and no further conditions on the probabilistic properties of the experimental time series is required. For this reason, all the discussed symmetry-related issues remain valid also in case of non-ergodic phenomena, but they must be necessarily interpreted on an ensemble basis, considering a suitably large number of experimental runs.

From a theoretical point of view, the definition of the SSRP provides a convenient mathematical schema for representing the pressure field and the FPUL acting on a symmetric cylinder oriented with zero angle-of-attack in a statistically-symmetric flow.

Form a practical point of view, the principles here described may provide relevant tools for the validation of wind-tunnel tests carried out in nominally-symmetric conditions, as well as establish a consistent theoretical framework for some common operations required during the fine-tuning of the experimental setup.

ACKNOWLEDGEMENTS

The experimental data used in the paper were obtained at Shimizu Corporation as documented in [9]. The scientific support offered by Prof. Yukio Tamura and the work of all the researchers involved in mentioned project is gratefully acknowledged.

REFERENCES

[1] T.A. Reinhold. Distribution and correlation of dynamic wind loads. *Journal of Engineering Mechanics*, ASCE, **109**(12), 1419-1436, 1983.

[2] A. Tallin and B. Ellingwood. Wind induced lateral-torsional motion of buildings. *Journal of Structural Division*, ASCE, **114**(9), 2085-2108, 1985.

[3] S.T. Thoroddsen, J.A. Peterka and J.E. Cermak. Correlation of components of wind-loading on tall buildings. *Journal of Wind Engineering and Industrial Aerodynamics* **28**, 351-360, 1988.

[4] M.S. Islam, B. Ellingwood and R.B. Corotis. Dynamic response of tall buildings to stochastic wind load. *Journal of Structural Engineering*, ASCE **116**(11), 2982-3002, 1990.

[5] A. Makino and Y. Mataki. Combination method of maximum response in consideration of statistical correlation of wind forces acting on high-rise building. Study on rectangular section models. Report No. 10909825, NASA Technical Memorandum, May 1994, pp. 257-266.

[6] Y. Tamura, H. Kikuchi and K. Hibi. Quasi-static wind load combinations for low- and middle-rise buildings. *Journal of Wind Engineering and Industrial Aerodynamics*, **91**(12-15), 1613-1625, 2003.

[7] N. Lin, C. Letchford, Y. Tamura, B. Liang and O. Nakamura. Characteristics of wind forces acting on tall buildings. *Journal of Wind Engineering and Industrial Aerodynamics*, **93**, 217-242, 2005.

[8] J. Kanda and H. Choi. Correlating dynamic force components on 3-D cylinders. *Journal of Wind Engineering and Industrial Aerodynamics*, **41**-**44**, 785-796, 1992.

[9] H. Kikuchi, Y. Tamura, H. Ueda, K. Hibi. Dynamic wind pressure acting on a tall building model - Proper orthogonal decomposition. *Journal of Wind Engineering and Industrial Aerodynamics*, **69**–**71**, 631–646, 1997.

[10] G. Solari, L. Carassale, F. Tubino. Proper Orthogonal Decomposition in Wind Engineering: Part 1: A State-of-the-Art and Some Prospects. *Wind & Structures*, **10**(2), 177-208, 2007.

[11] M.M. Zdravkovich. *Flow around circular cylinders Vol. 1: Fundamentals.* Oxford University Press, 1997.